Available online at www.sciencedirect.com
ScienceDirect
Journal of Molecular Graphics and Modelling 25 (2007) 773–783
Journal of Molecular Graphics and Modelling
www.elsevier.com/locate/JMGM

Exploring the molecular basis of the enantioselective binding of penicillin G acylase towards a series of 2-aryloxyalkanoic acids: A docking and molecular dynamics study

Antonio Lavecchia [a,*], Sandro Cosconati [a], Ettore Novellino [a], Enrica Calleri [b], Caterina Temporini [b], Gabriella Massolini [b], Giuseppe Carbonara [c], Giuseppe Fracchiolla [c], Fulvio Loiodice [c]

[a] *Dipartimento di Chimica Farmaceutica e Tossicologica, Università di Napoli "Federico II", Via D. Montesano, 49, I-80131 Napoli, Italy*
[b] *Dipartimento di Chimica Farmaceutica, Università di Pavia, Via Taramelli 12, I-27100 Pavia, Italy*
[c] *Dipartimento Farmaco-Chimico, Università di Bari, Via Orabona 4, I-70126 Bari, Italy*

Received 17 February 2006; received in revised form 4 July 2006; accepted 5 July 2006
Available online 8 August 2006

Abstract

In the present paper, molecular modeling studies were undertaken in order to shed light on the molecular basis of the observed enantioselectivity of penicillin G acylase (PGA), a well known enzyme for its industrial applications, towards 16 racemic 2-aryloxyalkanoic acids, which have been reported to affect several biological systems. With this intention docking calculations and MD simulations were performed. Docking results indicated that the (*S*)-enantiomers establish several electrostatic interactions with SerB1, SerB386 and ArgB263 of PGA. Conversely, the absence of specific polar interactions between the (*R*)-enantiomers and ArgB263 seems to be the main reason for the different binding affinities observed between the two enantiomers. Results of molecular dynamics simulations demonstrated that polar interactions are responsible for both the ligand affinity and PGA enantiospecificity. Modeling calculations provided possible explanations for the observed enantioselectivity of the enzyme that rationalize available experimental data and could be the basis for future protein engineering efforts.

Keywords: Docking; Enantioselectivity; Molecular dynamics; Molecular modeling; Penicillin G acylase

1. Introduction

The natural world is characterized by the presence of chiral compounds such as amino-acids and carbohydrates. These molecules are composed of units all having the same chiral configurations: the 21 essential amino acids are all *L*-enantiomers, while most carbohydrates have the D-configuration. Thus, critical physiological processes are homochiral, showing 100% stereoselectivity, and only involve one of all the possible stereoisomers of key molecules [1]. In this context, also when exogenous chiral compounds such as drugs are introduced in the body, physiological processes display a high degree of enantioselection [2], with the stereoisomers having very dissimilar effects on chiral targets (receptors, enzymes and ion channels), due to their diverse drug/target interactions. In fact, although enantiomers have identical chemical and physical properties in achiral environments, except for the property of rotation of polarized light, they can exhibit different physiological and biochemical behaviour in a chiral biological environment and may also have different pharmacodynamic and pharmacokinetic activities. Furthermore, the enantiomers of chiral drugs may display considerable differences in toxicity [3], as underscored by the tragedy of thalidomide in the early 1960s. In fact, the inactive isomer of this sedative and antinausea compound was found to be responsible for the teratogenic effects.

In this scenario, drug chirality has become one of the major issues in the design, discovery and development of new drugs [4–8]. In fact, in the last decades, the demand of enantiomerically pure drugs has increased together with their introduction

* Corresponding author. Tel.: +39 081678613; fax: +39 081678613.
E-mail address: lavecchi@unina.it (A. Lavecchia).

1093-3263/$ – see front matter © 2006 Elsevier Inc. All rights reserved.
doi:10.1016/j.jmgm.2006.07.001

in the market (from 20% 10 years ago to 75% nowadays). Therefore, the enantiomeric separation and analysis of chiral drugs turned out to be indispensable for chemists. Actually, several experimental procedures exist to separate racemates and, among them, the high-performance liquid chromatography (HPLC) seems to be the most commonly used technique. This approach can be divided into three main types: (i) direct separation (direct method) on a chiral stationary phase (CSP), (ii) separation on an achiral stationary phase by adding a chiral agent to the mobile phase, which then forms adducts with the enantiomeric analytes (chiral mobile phase additive method), and (iii) separation of the diastereomers formed by pre-column derivatization with a chiral derivatization reagent (CDR) (indirect method) [9]. Among these, protein-based CSPs are of special interest because of their unique enantioselective properties and because they are suitable for separating a wide range of enantiomerically pure compounds [10,11]. CSPs examples include albumins such as bovine and human serum albumins, glycoproteins such as α_1-acid-glycoprotein, ovomucoid, avidin and riboflavin binding protein, enzymes such as α-chymotrypsin, cellobiohydrolase I, lysozyme, pepsin, and other proteins [12]. Another enzyme, the penicillin G acylase (PGA), has been recently employed to develop a chiral stationary phase (PGA-CSP) [13–15]. This enzyme is well known for its industrial application in the production of the β-lactamic nucleus and for its enantioselectivity in the hydrolysis of amide or ester bonds [16]. PGA has also proven to be almost unbeatable in separating racemates because of its high enantioselectivity and broad ligand tolerance. Most precisely, several experiments clearly indicated that immobilized PGA can be successfully used as chiral selector for acidic compounds [17], such as 2-aryloxyalkanoic acids, isosteric analogous and some 2-arylpropionic acids [18]. The absolute configuration of these compounds has been shown to exert a strong influence in activating the peroxisome proliferator activated receptors (PPARs) [19,20], in allosterically modulating haemoglobin activity [21], in changing the skeletal muscle membrane chloride conductance [22,23], in modulating the prostaglandin-dependent platelet aggregation [24], and in inhibiting the cyclooxygenase enzyme [25].

Recently, the X-ray structures of PGA complexed with a series of phenylacetic acid analogues [26] and with penicillin G/penicillin G sulphoxide ligands [27] were solved, shedding light on the functional properties of PGA and on its catalytic mechanism. PGA belongs to the newly recognized structural superfamily of N-terminal nucleophile (Ntn) amidohydrolases [28]. The other Ntn hydrolases identified so far are the aspartylglucosaminidase (AGA) [29], proteasome (PRO) [30], and glutamine-PRPP-amidotransferase (GAT) [31]. The enzymes of this superfamily share similar three-dimensional folds and have analogies in their functional mode. They also have similar architectures of their active sites with corresponding catalytic elements arranged in analogous ways [28]. The binding site of PGA has been found to consist of three major regions that are responsible for the ligand recognition by the enzyme: the catalytic residue SerB1, the oxyanion hole (stabilizing the negative charge present on the ligand carboxylate group) formed by GlnB23, AlaB69, AsnB241 and a hydrophobic pocket which is able to accommodate lipophilic groups [26,27,32].

Considering the biological importance of the above cited acidic compounds and the potential industrial application of PGA as a chiral selector for a wide range of molecules, herein we performed a computational study in order to gain major insights into the molecular basis of the stereoselective binding of the enzyme towards a series of previously reported 2-aryloxy-2-aryl-acetic acids (**1**–**16**) (Table 1) [33].

Table 1
Chemical structures of the synthesized 2-aryloxy-2-aryl-acetic acid derivatives **1**–**16**, chromatographic parameters and differential free energy of binding

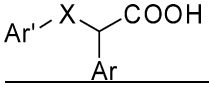

Analyte	X	Ar′	Ar	k_1[a]	α	R_s	$\Delta_{1,2}\Delta G$[b] (kcal/mol)
1	O	4-Cl-Ph	Ph	1.35 (*S*)[c]	2.24	2.16	−0.477
2	O	Ph	Ph	0.36	1.00	–	–
3	O	Ph	4-Cl-Ph	1.12 (*R*)	1.21	0.47	−0.113
4	S	Ph	4-Cl-Ph	2.22	1.19	0.43	−0.103
5	O	4-Cl-Ph	2-Cl-Ph	2.52	3.55	3.76	−0.750
6	O	4-Cl-Ph	4-Cl-Ph	5.58	1.00	–	–
7	O	4-Cl-Ph	4-CF_3-Ph	12.27	1.58	1.84	−0.271
8	O	4-Cl-Ph	4-CH_3-Ph	2.47	1.00	–	–
9	O	4-Cl-Ph	4-CH_3O-Ph	1.90	1.11	0.47	−0.062
10	O	4-Cl-Ph	4-*i*-Pr-Ph	7.78	1.00	–	–
11	O	4-Cl-Ph	4-Ph-Ph	40.66	1.14	0.54	−0.078
12	O	Ph	1-Naph	4.57 (*R*)	1.92	2.50	−0.386
13	O	4-Cl-Ph	1-Naph	8.57	2.81	3.49	−0.611
14	O	2,6-Cl_2-Ph	Ph	0.87	1.00	–	–
15	O	4-CH_3O-Ph	Ph	0.53	1.00	–	–
16	O	2-Naph	Ph	4.64 (*R*)	1.17	0.51	−0.093

[a] k_1 is the retention factor of the first eluted enantiomer.
[b] Differential free energy of binding calculated from the chromatographic data.
[c] Absolute configuration of the less retained enantiomer.

With this purposes, the 3D-structure of PGA solved through X-ray crystallography (PDB Entry Code: 1AJN) [26] was used to dock both isomers of titled compounds through the automated docking program AutoDock [34], which has been shown to be predictive in reproducing experimentally observed binding poses [35]. The predicted binding conformations were subsequently used as input for molecular dynamics (MD) simulations using the software Q [36] in order to inspect the ligand/enzyme binding interactions from a dynamical point of view and to calculate the energetic contribution to the binding of the selected compounds. Q implements the linear interaction energy (LIE) method to calculate the ligand binding affinities [37–39], which has proven to be successful for a number of different systems as reported by several papers by Åqvist and co-workers [40–43].

2. Computational methods

2.1. Docking

Docking simulations were carried out using AutoDock 3.0.5 version [34]. It combines a rapid energy evaluation through pre-calculated grids of affinity potentials with a variety of search algorithms to find suitable binding positions for a ligand on a given protein. While the protein is required to be rigid, the program allows torsional flexibility in the ligand. Docking of both (*R*)- and (*S*)-enantiomers of compounds **1**–**16** to PGA was carried out using the empirical free energy function and the Lamarckian genetic algorithm (LGA) [34], applying a standard protocol, with an initial population of 50 randomly placed individuals, a maximum number of 1.5×10^6 energy evaluations, a mutation rate of 0.02, a crossover rate of 0.80, and an elitism value of 1. Proportional selection was used, where the average of the worst energy was calculated over a window of the previous 10 generations. For the local search, the so-called pseudo-Solis and Wets algorithm was applied using a maximum of 300 iterations per local search. The probability of performing local search on an individual in the population was 0.06, and the maximum number of consecutive successes or failures before doubling or halving the local search step size was 4.50 independent docking runs were carried out for each ligand. Results differing by less than 1 Å in positional root-mean square deviation (rmsd) were clustered together and represented by the result with the most favourable free energy of binding (ΔG_{bind}).

2.2. Ligand setup

The structures of the ligands **1**–**16** were generated using standard bond lengths and bond angles of the SYBYL fragment library [44]. Geometry optimizations were conducted with the SYBYL/MAXIMIN2 minimizer by applying the BFGS (Broyden, Fletcher, Goldfarb and Shannon) algorithm [45] with a convergence criterion of 0.001 kcal/mol Å and employing the TRIPOS force field [46]. Partial atomic charges were assigned using the Gasteiger–Marsili formalism [47], which is the type of atomic charges used in calibrating the AutoDock empirical free energy function. Finally, the compounds were setup for docking with the help of AutoTors, the main purpose of which is to define the torsional degrees of freedom to be considered during the docking process. All torsion angles for each inspected compound were considered flexible.

2.3. Protein setup

The crystal structure of PGA in complex with *p*-nitrophenylacetic acid (entry code: 1AJN) [26], recovered from Brookhaven Protein Database [48], was used. In AutoDock, the polar hydrogens are explicitly treated, while the non-polar hydrogens are "unified" with their parent heavy atoms, by increasing the heavy atom's van der Waals' radius. Therefore, the structure was set up for docking as follows: polar hydrogens were added using the BIOPOLYMERS module within SYBYL program (residues Arg, Lys, Glu, and Asp were considered ionized, while all His were considered neutral by default) and Kollman united-atom partial charges were assigned. The grid maps representing the proteins in the actual docking process were calculated with AutoGrid. The grids (one for each atom type in the ligand, plus one for electrostatic interactions) were chosen to be sufficiently large to include not only the active site but also significant portions of the surrounding surface. The dimensions of the grids were thus 60 Å × 60 Å × 60 Å, with a spacing of 0.375 Å between the grid points. The centre of the grid was set to be coincident with the mass centre of the ligand in the crystal complex.

Figs. 2–4 of the calculated binding modes for compounds (*S*)-**3**, (*R*)-**3**, (*S*)-**11**, (*R*)-**11**, (*S*)-**12** and (*R*)-**12** were made using PYMOL software [49].

2.4. MD and binding free energy calculation

The software Q [36] was employed for the MD simulations and analysis selecting the force field parameters of AMBER parm94 implemented in the program [50]. This force field was modified to include additional parameters for each inspected ligand. Most of these parameters were adapted by analogy from others included in the AMBER parm94 force field and the missing ones were taken from those reported in literature [51]. Partial charges for each ligand were derived from the semi-empirical quantum mechanics AM1-BCC method. The choice of this method was dictated by the fact that results are very similar to those obtained from widely used RESP charges in the AMBER force field [52,53]. The values were adjusted to be compatible with the AMBER force field by scaling the QM charges to match the values for groups defined in the force field library and by slight modifications to achieve electroneutral groups of less than about 10 atoms. In both the bound and the free states, the ligand was solvated with TIP3P [54] water sphere of 18 Å radius. In the MD simulation of the solvated ligand–protein complexes, ionic groups of the protein within the water sphere that were far away from the boundary were modeled as charged (SerB1 N-terminal and ArgB263). The resulting net charge for the sphere of simulation was +2, since

there were no Glu or Asp residues that could be ionized to counterbalance negative charges.

The system was initially submitted to a stepwise warm-up and equilibration procedure consisting of blocks of 4 ps at 0, 50, 100, 150, and 300 K, while the bath coupling was relaxed from τ = 1–5 fs, with all heavy solute atoms weakly restrained to their initial positions (5 kcal mol^{-1} Å^{-2}). Productive MD simulations for the data collection were performed at 300 K (coupling to the temperature bath was set to t = 10 fs) with a time step of 1 fs. A 10 kcal mol^{-1} Å^{-2} force constant was imposed on the atoms in the boundary zone between 16.5 and 18 Å from the sphere centre. All the protein atoms inside that sphere and all ligand atoms were completely free to move, while the protein atoms outside the sphere of simulation were fixed by a high (100 kcal mol^{-1} Å^{-2}) harmonic constraint.

In the free simulation, the ligands were solvated in a 18 Å radius water sphere and were relaxed through 2 ps MD with a bath coupling (τ) of 0.2 fs followed by 5 ps at temperature of 300 K, applying a harmonic constraint of 10 kcal mol^{-1} Å^{-2} on all ligand atoms. In this stage, the central atom of the ligand was geometrically restrained to the centre of the grid by use of a 50 kcal mol^{-1} Å^{-2} force constant, to ensure a homogenous solvation. Time step and bath coupling were set to the same values as in the bound state. Analysis of the MD results was achieved with the tools present in the Q software package. Fig. 5 of the complex between (*S*)-**5**, PGA and solvating waters used as input for MD simulations was made using PYMOL software [49].

3. Results

3.1. Docking studies

With the recent developments in search algorithms and energy functions, computational docking methods have become a helpful device to investigate ligand–protein interactions in the absence of detailed experimental data and can contribute to the understanding of its structural and energetic basis. Among all docking software, AutoDock has been shown to be predictive in reproducing experimentally observed binding modes using an empirical free energy function and a Lamarckian genetic search (LGA) algorithm [34,35]. For docking calculations, the crystal structure of PGA in complex with the 2-(4-nitrophenyl)acetic acid (PDB entry-code: 1AJN) [26], was employed.

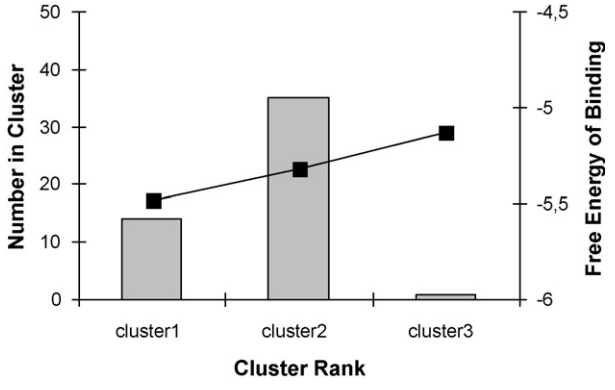

Fig. 1. AutoDock results for docking of 2-(4-nitrophenyl)acetic acid into the PGA enzyme.

Prior to automated docking of the reported ligands, 2-(4-nitrophenyl)acetic acid itself was docked into the PGA crystal structure as a means of testing program performance. The docking test indicated that the largest cluster (cluster 2 in Fig. 1) of similar conformations with an estimated ΔG_{bind} of −5.32 kcal/mol reproduced very closely the crystallographic binding mode of the 2-(4-nitrophenyl)acetic acid. The H-bonds predicted by AutoDock were virtually identical to those found in the crystal structure.

Thus, both (*R*)- and (*S*)-enantiomers of compounds **1**–**16** (Table 1) were subjected to docking simulations. We decided to begin our inspection with all those compounds in which the racemate was efficiently separated into the two enantiomers by the enzyme. Moreover, docking was also conducted for those compounds displaying poor enantioselective separation in an attempt to elucidate the reasons behind the reduced enantiodiscrimination. For all investigated compounds well-clustered

Table 2
Result of 50 independent docking runs for each ligand

Compounds	N_{tot} [a]	f_{occ}	ΔG_{bind}
(*S*)-**1**	41	4	−5.80
(*R*)-**1**	44	3	−5.55
(*S*)-**2**	17	9	−6.80
(*R*)-**2**	19	10	−6.98
(*S*)-**3**	17	23	−7.08
(*R*)-**3**	24	9	−6.48
(*S*)-**4**	21	15	−7.58
(*R*)-**4**	25	6	−7.09
(*S*)-**5**	16	25	−7.13
(*R*)-**5**	16	22	−6.03
(*S*)-**6**	11	23	−7.50
(*R*)-**6**	14	15	−7.47
(*S*)-**7**	20	16	−8.01
(*R*)-**7**	13	31	−7.33
(*S*)-**8**	35	6	−6.17
(*R*)-**8**	38	4	−5.99
(*S*)-**9**	23	15	−7.03
(*R*)-**9**	26	8	−6.75
(*S*)-**10**	26	3	−7.37
(*R*)-**10**	28	3	−7.26
(*S*)-**11**	9	36	−9.43
(*R*)-**11**	16	16	−8.92
(*S*)-**12**	18	17	−8.57
(*R*)-**12**	25	8	−7.85
(*S*)-**13**	20	20	−9.07
(*R*)-**13**	19	16	−8.16
(*S*)-**14**	20	5	−6.86
(*R*)-**14**	24	6	−6.77
(*S*)-**15**	15	15	−6.35
(*R*)-**15**	22	7	−6.54
(*S*)-**16**	18	12	−7.14
(*R*)-**16**	25	5	−6.48

[a] N_{tot} is the total number of clusters; the number of results in the most populated cluster is given by the frequency of occurrence, f_{occ}; ΔG_{bind} is the estimated free energy of binding for the cluster with the highest f_{occ} and is given in kcal/mol.

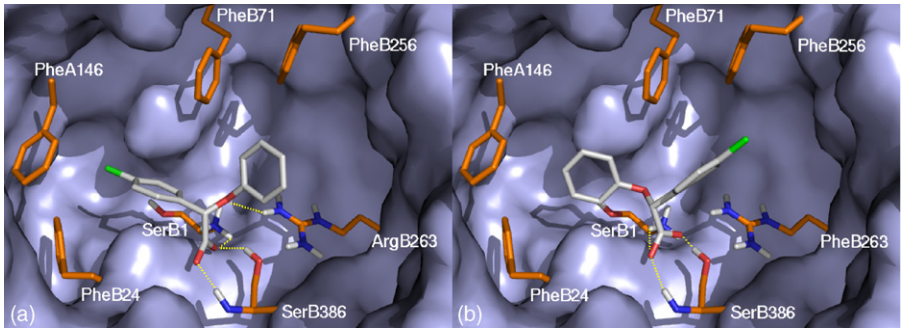

Fig. 2. Binding mode of compound (*S*)-**3** (a) and (*R*)-**3** (b) within PGA. For clarity reasons only interacting residues are displayed. Hydrogen bonds between ligand and protein are shown as dashed yellow lines. Ligand (white) and interacting key residues (orange) are represented as stick models, while the protein as a light grey Connolly surface.

docking results could be obtained. The 50 independent docking runs carried out for each ligand generally converged to a small number of different positions clusters. Generally, the top ranking clusters (i.e. those with the most favourable ΔG_{bind}) were also associated with the highest frequency of occurrence, which suggests a good convergence behaviour of the search algorithm. The best results in terms of free energy of binding were all located in a similar position in the active site. Docking results (the total number of clusters, the number of results in the most populated cluster and the relative estimated free energy of binding) are summarized in Table 2, and a graphical representation of the binding modes of the most structurally representative derivatives (*S*)-**3**, (*R*)-**3**, (*S*)-**11**, (*R*)-**11**, (*S*)-**12** and (*S*)-**11**, is given in Figs. 2–4. Results are briefly described in the following section.

3.1.1. Compounds 3–5

A distinct binding pose was found for (*S*)-**3**, (*S*)-**4** and (*S*)-**5**. As depicted in Fig. 2a, the associated binding mode for (*S*)-**3** is characterized by the presence of numerous H-bond interactions involving the carboxylate group with both the backbone NH and the OH group of SerB386. An additional H-bond is established between the ether oxygen of the ligand and the ArgB263 side chain. Moreover, an ionic interaction is formed between the negatively charged carboxylate group and the positively charged N-terminal SerB1. A set of charge-transfer interactions is also found between the ligand phenoxy and phenyl moieties and the PheB24, PheA146, PheB71 and PheB256 aromatic rings. A similar binding pose was also found for (*S*)-**4** with the same polar and charge transfer interactions. Interestingly the sulphur atom is still able to H-bond with ArgB263 side chain. Also for (*S*)-**5** the best docked solution resembles the (*S*)-**3** one.

Regarding (*R*)-**3**, (*R*)-**4** and (*R*)-**5**, the calculated posing is similar to the one found for the (*S*)-isomer, even if the H-bond interaction between the ether oxygen and ArgB263 side chain is absent and the phenoxy moiety is placed in the same position occupied by the phenyl ring in the (*S*)-compounds (Fig. 2b).

The poor docking run convergence (Table 2), the high estimated ΔG_{bind} and the absence of the H-bond interaction with ArgB263 would suggest that (*R*)-isomers of **3** and **4** form a less stable complex with PGA. Such a result is in accordance with experimental data indicating that (*R*)-**3** is the first to be eluted by the stationary phase. Noticeably, for both enantiomers of **4**, the experimentally found k_1 and k_2 values are lower than those of (*R*)-**3** and (*S*)-**3**. It could be speculated that the sulphur atom, being more lipophilic, establishes supplemental favourable hydrophobic contacts with the enzyme.

3.1.2. Compounds 7 and 9

Comparable results were obtained for compounds (*S*)-**7** and (*S*)-**9** with the binding pose strongly resembling those observed for the (*S*)-isomers of the compounds described so far. A prevailing posing was also found for (*R*)-**7** and (*R*)-**9**. However, the predicted conformation lacks of the recurring set of interactions formerly found.

3.1.3. Compound 11

As regards enantiomer (*S*)-**11**, a single top ranking cluster was calculated by AutoDock. As shown in Fig. 3a, the structure

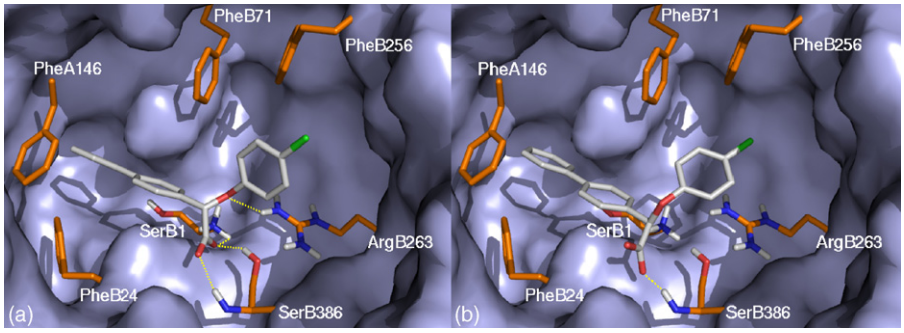

Fig. 3. Binding mode of compound (*S*)-**11** (a) and (*R*)-**11** (b) within PGA.

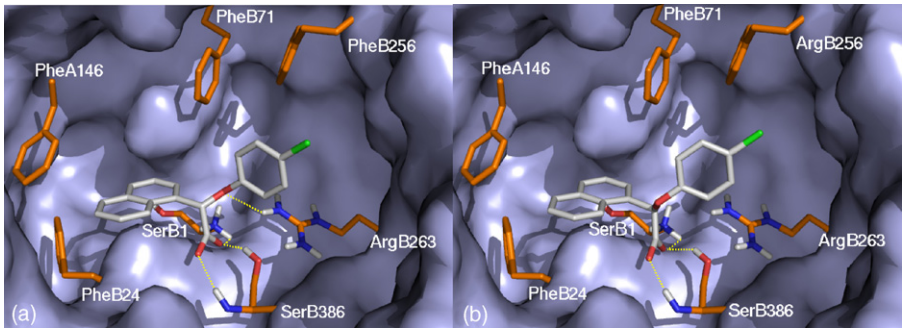

Fig. 4. Binding mode of compound (*S*)-**12** and (*R*)-**12** within PGA.

of the ligand fits into the binding cavity similarly to (*S*)-**3** with the biphenyl and *p*-Cl-phenoxy groups involved in numerous charge-transfer interactions with PheB256, PheB71, PheB24 and PheA146. As calculated by AutoDock, (*R*)-**11** occupies the same space as the (*S*)-isomer, even though the carboxylate group is unable to establish the commonly found polar interactions with the PGA (Fig. 3b). The different values of ΔG_{bind} observed for both isomers of **11** suggest that the (*S*)-enantiomer should be more retained by the stationary phase than the (*R*)-one.

3.1.4. Compounds *12* and *13*

Docking of (*S*)-**12** and (*S*)-**13** into the PGA resulted in a posing resembling the ones reported for the (*S*)-enantiomers described so far (Fig. 4a). From a visual inspection of the predicted binding poses of (*S*)-**12** and (*S*)-**13**, the phenyl and naphthalene rings establish charge-transfer interactions with PheB71, PheB256, PheB24 and PheA146 side chains.

The calculated binding modes of both (*R*)-**12** and (*R*)-**13** are similar to that observed for the respective (*S*)-isomers, excepted for the absence of the H-bond interaction between the ether oxygen and the ArgB263 side chain (Fig. 4b). Therefore, it seems plausible to suppose that the (*S*)-enantiomers of these compounds, which form a more stable complex with PGA, are more retained by the stationary phase according with what reported by Massolini et al. [33]. In fact, compound **12** was synthesized in enantiomeric form confirming that the elution order was *R*:*S*. Moreover, it is worth noting that the k_1 value for both enantiomers of **13** are fairly higher if compared with those of previously analyzed compounds, which suggests that PGA forms a stable complex with both enantiomers of **13**. This could be explained by the presence of the *p*-Cl group on the phenoxy moiety. In fact, the electron-deficient halogenated ring would more favourably realize charge-transfer interactions with the electron-rich ring of aromatic amino acids into the PGA binding site.

3.1.5. Compounds *14–16*

For both isomers of **14**, AutoDock failed in predicting a single and highly populated cluster, which indicates that several different binding modes are feasible for these enantiomers. This is in agreement with the chromatographic experiments, which display that the stationary phase scarcely retains compound **14** ($k_1 = 0.87$) and is unable to discriminate between both enantiomers ($\alpha = 1$). A single cluster was obtained for (*S*)-**15** and (*S*)-**16** with the top ranking results featuring the same interactions found for (*S*)-enantiomers of previously described compounds. Less convergent results were obtained for both (*R*)-**15** and (*R*)-**16**. The associated binding modes resemble the (*S*) ones, although the H-bond between the ether oxygen and the ArgB23 side chain is absent. It is worth noting that for both enantiomers of **15** low experimental k_1 values were found. This behaviour might be explained with the presence of the electron-donating *p*-OMe group on the phenoxy moiety, which weakens the charge transfer interactions with PheB71 and PheB256. Concerning compound **16**, docking results agree with the elution order *R*:*S* found in the chromatographic experiments.

3.1.6. Compounds *2* and *6*

Peculiar results were obtained for both (*R*)- and (*S*)-isomers of **2** and **6**. In fact, AutoDock found two possible binding poses in which the phenoxy and phenyl groups were interchangeable. The associated ΔG_{bind} values are comparable for each predicted binding mode, thus, suggesting that PGA is unable to discriminate between the two enantiomers.

3.1.7. Compounds *1*, *8* and *10*

Docking of both (*R*)- and (*S*)-isomers of **1**, **8** and **10** into the PGA binding pocket did not converge towards a single binding position. From a visual inspection of the ligand/PGA complex it seems clear that the steric hindrance of bulky *i*-propyl group in **10** prevents both enantiomers from adapting themselves into the stereoselective PGA binding. Regarding ligands **1** and **8**, only poorly populated clusters are calculated for both enantiomers of each compound. This indicates that several different binding modes are feasible; hence a direct comparison between computational and experimental data seems unviable.

3.2. Molecular dynamics simulations

When predicting the posing of a ligand into a protein, docking can provide a good starting point for further calculations with the aim of evaluating the stability of the predicted interactions involved in binding. In this respect, MD simulations were undertaken to consider the effects of the receptor flexibility and the explicit water solvation on the complex of interest. In this study, the employment of the software Q [36], which implements the LIE method, also

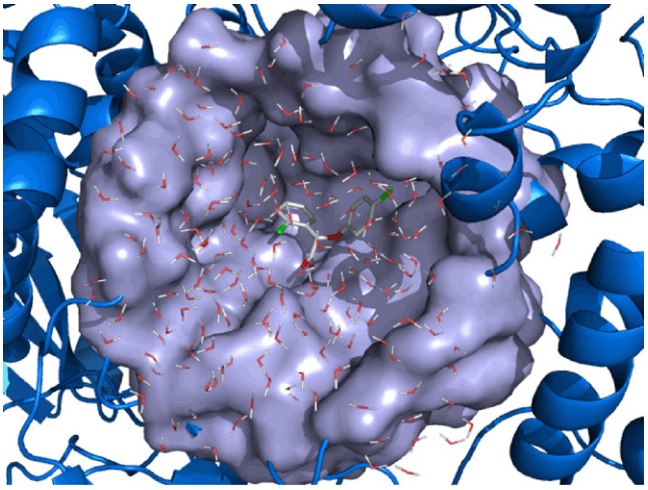

Fig. 5. Complex between (*S*)-**5**, PGA and solvating waters used as input for MD simulations. PGA is represented as blue ribbon while residues within 18 Å (free to move) from the ligand are represented as light grey Connolly surface. Ligand and water molecules are represented as sticks (carbon atoms white, oxygens red and chlorine atoms in green).

allowed to estimate the ΔG_{bind} values from MD simulation averages of the non-bonded intermolecular ligand potential energies [37,55]. Most precisely, this approach is based on thermal conformational sampling of the ligand, both in the free state (i.e., solvated in water) and bound to the solvated protein. The estimated energy of binding is calculated as a linear combination of the differences in the average ligand–environment interactions. In the bound state, the environment is represented by both the protein and the solvating water molecules (see Fig. 5), while in the unbound state, the environment is represented by the only water molecules.

The interaction energies are divided into an electrostatic term and a van der Waals term as described in the following equation:

$$\Delta G_{calc} = \alpha(\langle V_{l-s}^{vDW}\rangle_p - \langle V_{l-s}^{vDW}\rangle_w) + \beta(\langle V_{l-s}^{el}\rangle_p - \langle V_{l-s}^{el}\rangle_w) + \gamma \quad (1)$$

where the terms $\langle V_{l-s}\rangle$ represent the thermal averages calculated over the MD simulations of the electrostatic (el) and van der Waals (vdW) energies for the ligand atoms in the bound (p) state and in the free (w) state. Since our ligands are negatively charged, we used a β value of 0.5 for the electrostatic interactions [56], and a α value of 0.181 for the non-polar interactions [57]. The constant parameter $\gamma \neq 0$ can be adjusted by least-squares optimization in order to improve the calculated absolute binding energies quantitatively with respect to the experimental ones. In the present inspection, we did not optimize this parameter, since we were mainly interested in calculating a relative binding free energy.

With the above-mentioned approach, we achieved the ΔG_{bind} for the most enantiodiscriminated compounds **3**–**5**, **7**, **12** and **13**. No calculations were conducted on compound **1**, since AutoDock failed in predicting a well-defined binding conformation to use as input for MD simulations. Also the scarcely enantiodiscriminated **9**, **11** and **16** were excluded from this inspection (see $\Delta_{1,2}\Delta G$ values in Table 1). Results of MD simulations are summarized in Table 3.

Table 3
LIE average ligand-surroundings interaction energies (kcal/mol) for compounds **3**–**5**, **7**, **11**–**13**, **16** in water and in the protein together with the calculated binding free energies

Analyte	Water		Protein		ΔG_{bind} (kcal/mol)
	$\langle V_{l-s}^{el}\rangle_w$	$\langle V_{l-s}^{vdW}\rangle_w$	$\langle V_{l-s}^{el}\rangle_p$	$\langle V_{l-s}^{vdW}\rangle_p$	
(*S*)-**3**	−141.25	−17.44	−216.83	−28.43	−39.78
(*R*)-**3**	−141.72	−17.16	−216.71	−28.54	−39.55
(*S*)-**4**	−138.46	−17.33	−214.36	−29.03	−40.07
(*R*)-**4**	−138.80	−17.50	−214.39	−28.84	−39.83
(*S*)-**5**	−136.70	−18.36	−214.40	−30.54	−41.05
(*R*)-**5**	−138.02	−18.24	−210.73	−30.63	−38.59
(*S*)-**7**	−137.83	−24.73	−211.23	−39.04	−39.29
(*R*)-**7**	−138.37	−24.58	−210.30	−40.32	−38.81
(*S*)-**12**	−138.62	−22.03	−218.752	−37.06	−42.78
(*R*)-**12**	−138.13	−22.12	−214.03	−36.46	−40.54
(*S*)-**13**	−139.50	−22.54	−219.72	−37.37	−42.79
(*R*)-**13**	−138.13	−23.16	−215.57	−36.59	−41.15

No direct correlation between experimental and calculated ΔG_{bind} was attempted because of the small chromatographic differential free energy of binding ($\Delta\Delta G_{bind}$) (up to 0.7 kcal/mol). In fact, it has been reported that generally the final error of the converged Q/LIE free energy simulations was about 2 kcal/mol, which is much higher than the experimental values we had [41].

During the MD simulations all compounds remained in a stable binding position with low rmsd (root-mean square deviations) fluctuations, thus, confirming the feasibility of the binding poses predicted by AutoDock. In addition, LIE calculations were helpful in gaining major insights into the main reasons responsible for the observed enantioselectivity

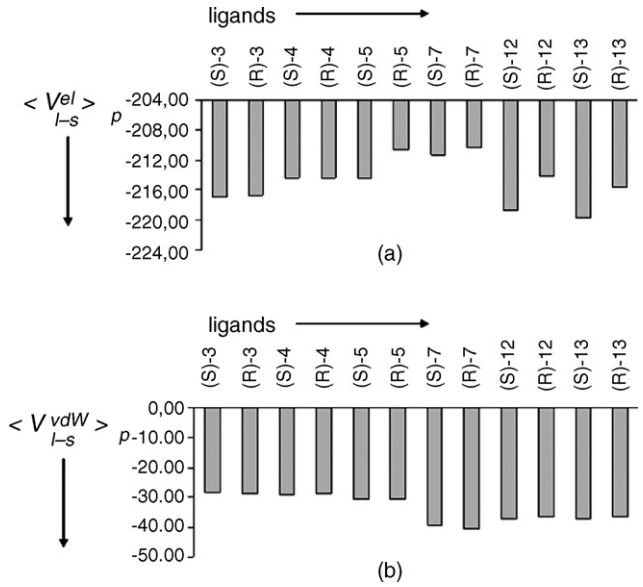

Fig. 6. Plot of the of the electrostatic (a) and van der Waals (b) energy contributions for the ligand atoms in the bound state for both enantiomers of compounds **3**–**5**, **7**, **12** and **13** as calculated by MD simulations with Q/LIE.

of PGA towards the inspected ligands. In fact, analysis of the non-bonded interactions (electrostatic and van der Waals) between the protein and compounds **3**–**5**, **7**, **12** and **13** (Fig. 6a and b) clearly show that polar rather that hydrophobic interactions mainly contribute to the binding of the inspected ligands. Moreover, by comparing the electrostatic contributions calculated for both isomers of each enantiopair, one can see that for the most enantiodiscriminated racemates, **5**, **7**, **12** and **13**, high differences between the (*R*)- and (*S*)-enantiomers were found (Table 4 and Fig. 6). Most precisely, the electrostatic energy of interaction in the (*R*)-enantiomer is generally higher than the corresponding one in the (*S*)-isomer. On the other hand, small differences between the isomers of each enantiopair were recorded for the van der Waals contribution.

4. Discussion

Knowledge of structures of enzyme/ligand complexes is indispensable (although not necessarily sufficient) to clarify the molecular details of the binding mechanism and to understand and perhaps be able to modify the selectivity of the binding recognition process. In this paper, molecular modeling studies were undertaken in order to provide a possible explanation at molecular level of the observed enantioselectivity of PGA towards a set of selected acidic compounds. To achieve this, docking experiments of both (*R*)- and (*S*)-enantiomers of acetic acid derivatives **1**–**16** were undertaken using the 3D crystal structure of PGA [26]. Interestingly, the automated docking program AutoDock found for the (*S*)-enantiomers of almost all compounds the same binding conformation characterized by a set of recurring interactions (Figs. 2–4). AutoDock found also a similar binding pose for the (*R*)-enantiomers of **3**–**5**, **7**, **9**, **11**–**13**, **15** and **16** as well as the same set of interactions, with the exception of the H-bond between the ligand ether oxygen and the ArgB263 side chain. Hence, the loss of such interaction might rationalize the chiral selecting behaviour displayed by this enzyme towards the analyzed training set. Such findings strongly agree with previous data indicating the crucial role of ArgB263 in the PGA ligand specificity and stereoselectivity [58]. As shown in Table 1, racemates **2** and **6** are not separated by this enzyme. Remarkably, our docking study confirmed these experimental results. In fact, for both enantiomers of these compounds, AutoDock calculated two isoenergetic binding modes in which the carboxylate group still remained anchored to the binding site interacting with SerB1 and SerB386 side chain, whereas the phenoxy and phenyl groups were interchangeable. As a result, PGA is unable to discriminate between the two isomers of **2** and **6**. It could be speculated that this enzyme fails in discriminating all those acetic acid derivatives in which the phenoxy and phenyl groups bear the same substituent in the same position.

Peculiar results were obtained when docking was performed on **10** and **14**, bearing bulkier groups or more than one substituent on the aromatic rings. Indeed, due to their steric hindrance, the *i*-propyl group in **10** and the two *o*-Cl atoms in **14** prevent these ligands from adapting themselves into the PGA stereoselective binding site, thus explaining why they are not efficiently separated by the enzyme.

As previously reported, docking was not helpful when trying to explain the unexpected behaviour of compound **1**, which displays a reversed elution order *S*:*R*. In the great majority of the separated compounds, the (*S*)-enantiomers adapt themselves in the stereoselective binding site establishing strong charge transfer interactions between their phenyl ring substituted with electron-withdrawing groups (**3**–**5** and **7**) or additional aromatic rings (**11**–**13**) and PheA146, PheB24 and PheB71. On the other hand, the predicted binding mode for the (*R*)-enantiomers places the phenoxy moiety in the same position occupied by the phenyl ring in the (*S*)-ligands, engaging the same sort of interactions. In compound **1**, the electron-withdrawing chlorine substituent is present on the phenoxy moiety while the phenyl ring is not substituted, thus it could be hypothesized that only the (*R*)-enantiomer is able to establish strong charge transfer interactions with the enzyme. This might explain the reversed elution order found for this compound.

The calculated posing was also useful in rationalizing the different retention factors observed for all analyzed compounds. It is worth noting that while polar interactions for all PGA/ligand complexes remain unvaried, charge-transfer interactions have a different strength depending on the electron-withdrawing or electron-donating substituent (compare k_1 of **8** versus **7** and **1** versus **15**). In fact, electron withdrawing substituents decrease the π-electron density in aromatic rings and subsequently the important π-electron repulsion, whereas electron donating substituents disfavour a π–π interaction, augmenting the π-electron density within the rings and, as a consequence, the π-electron repulsion [59–61]. The importance of charge-transfer interactions in the predicted binding poses is confirmed by the experimental data indicating an increase in retention of both (*R*)- and (*S*)-enantiomers for those compounds bearing electron-withdrawing substituents on Ar and/or Ar′. Indeed, compound **2**, bearing no substituents on Ar′ and Ar, is less retained by PGA-CSP than structurally similar compounds **1**, **3** and **6**.

Unfortunately, docking calculations have some intrinsic drawbacks when considering that the effect of solvating water molecules is not explicitly treated. Moreover, during the simulation the receptor remain fixed and it has been reported that the binding free energies can largely vary due to the protein motion [62]. Therefore, further calculations were undertaken performing MD simulations with the software Q [36], which implements the LIE method to calculate the binding affinities [37]. From a close analysis of the MD simulation results, it seems clear that the binding of all ligands into the PGA active site is clearly dominated by polar rather than hydrophobic interactions, as demonstrated by the high electrostatic terms which mainly contribute to the absolute binding affinity (see $\langle V^{el}_{l-s}\rangle_w$ versus $\langle V^{el}_{l-s}\rangle_p$ in Table 3). This is further confirmed when looking at the different frames obtained from MD simulations, in which the carboxylate group remains anchored to the protonated nitrogen atom of the N-terminal SerB1, also establishing H-bond interactions with both the backbone NH

and OH group of SerB386. Moreover, while in the (*S*)-enantiomers the ether oxygen H-bonds with ArgB263 side chain, in the (*R*)-ones this interaction is absent or fairly instable. From these considerations, it seems that polar interactions not only provide most of the overall affinity of these compounds for PGA, but are also responsible for the enantiospecificity of the enzyme. In fact, as reported in Table 4 and Fig. 6, the main differences in the ligand-surroundings interaction energies between the (*R*)- and (*S*)-enantiomers were only recorded for the electrostatic contributions in the bound state and not for the non-polar ones.

5. Conclusions

The goal of this study was to elucidate the reasons behind the enantioselective binding of a highly efficient chiral selector such as PGA towards a set of acidic compounds in which the absolute configuration has been reported to exert a strong influence on several biological systems [19–24]. Thus, the 3D-structure of the enzyme solved through X-ray crystallography [26] was used to dock both (*R*)- and (*S*)-isomers of **1**–**16** employing the automated docking software AutoDock. Docking results indicated that the (*S*)-enantiomers establish several polar interactions with SerB1, SerB386 and ArgB263 of PGA. Conversely, the absence of specific polar interactions between the (*R*)-enantiomers and ArgB263 seems to be the main reason for the different chromatographic retention factors observed between (*R*)- and (*S*)-enantiomers, thus, explaining the PGA enantioselective behaviour. Docking experiments were also helpful in rationalizing the absence of enantioselectivity observed for some tested compounds (**2**, **6**, **10**, **14** and **15**). In fact, the steric hindrance of bulky groups on the phenyl ring (**10**) or an additional substituent on the phenoxy portion (**14**) might prevent these ligands from adapting themselves into the stereoselective binding site of PGA. It could be speculated that this enzyme fails in discriminating all those acetic acid derivatives in which the phenoxy and phenyl groups bear the same substituent in the same position, as confirmed by docking of **2** and **6**. Moreover, this computational study underlines the importance of the numerous charge-transfer interactions established between the ligands and the enzyme. In particular, an increase in the electron-withdrawing effect on both aromatic rings might stabilizes the complex between the selected compounds and PGA leading to an increase of the retention factors. To evaluate the effect of the receptor plasticity on ligand binding together with the influence of the water solvation, MD simulations were performed employing the software Q [36]. This computational approach revealed to be really helpful in elucidating the molecular basis of the observed enantioselectivity of PGA towards the selected compounds. In fact, from an accurate analysis of MD results it seems clear that polar interactions provide most of the overall affinity of these compounds for PGA and are responsible for the enantiospecificity of the enzyme.

In principle, the predictive power of the presented theoretical approach could be assessed by performing a comparison between experimental and calculated parameters ($\Delta\Delta G_{calc}$ versus $\Delta\Delta G_{exp}$) to see if they quantitatively correlate. Indeed, such a correlation might be hampered by some limitations connected with the experimental procedure adopted. In fact, it is worth noting that the $\Delta\Delta G_{exp}$ values not only result from specific interactions with the enzyme active site but also from interactions with the protein at other binding sites and possibly also with the support. From this point of view, a quantitative correlation between $\Delta\Delta G_{calc}$ and $\Delta\Delta G_{exp}$ values would mean comparing different factors which make such a correlation somehow weak. However, even if the predictive power of the presented computational approach cannot unequivocally be assessed, the qualitative consistency of both docking and MD simulations results with chromatographic data suggests that our approach could be used to shed light on the reasons of the observed enantioselective binding behaviour of diverse biological targets. Moreover, the modeled complexes between the inspected chiral compounds and PGA form the basis for rational protein engineering efforts aimed at improving the enantioselectivity of PGA, thus, enhancing its industrial applications.

Acknowledgment

This work was supported by grant from Ministero dell'Università e della Ricerca Scientifica (grant no. 2002034857_003).

References

[1] W.A. Bonner, Parity violation and the evolution of biomolecular homochirality, Chirality 12 (2000) 114–126.
[2] I. Agranat, H. Caner, J. Caldwell, Putting chirality to work: the strategy of chiral switches, Nat. Rev. Drug Discov. 1 (2002) 753–768.
[3] H.Y. Aboul-Enein, L.I. Abou-Basha (Eds.), The Impact of Stereochemistry on Drug Development, and Use, Wiley, New York, NY, 1997.
[4] M. Eichelbaum, A.S. Gross, Stereochemical aspects of drug action and disposition, Adv. Drug Res. 28 (1996) 2–64.
[5] R. Crossley (Ed.), Chirality, and the Biological Activity of Drugs, CRC Press, Boca Raton, FL, 1995.
[6] D.J. Triggle, Stereoselectivity of drug action, Drug Discov. Today 2 (1997) 138.
[7] C.A. Challener (Ed.), Chiral Drugs, Ashgate Burlington, Vermont, 2001.
[8] M. Eichelbaum, B. Testa, A. Somogyi (Eds.), Stereochemical Aspects of Drug Action, Springer, Heidelberg, 2002.
[9] X.X. Sun, L.Z. Sun, H.Y. Aboul-Enein, Chiral derivatization reagents for drug enantioseparation by high-performance liquid chromatography based upon pre-column derivatization and formation of diastereomers: enantioselectivity and related structure, Biomed. Chromatogr. 2 (2001) 116–132.
[10] S. Allenmark (Ed.), Chromatographic Enantioseparation: Methods, and Applications, 2nd ed., Ellis Horwood, New York, 1991 (Chapter 7).
[11] I.W. Wainer (Ed.), Drug Stereochemistry: Analytical Methods, and Pharmacology, Marcel Dekker, New York, 1993 (Chapter 6).
[12] J. Haginaka, Protein-based chiral stationary phases for high-performance liquid chromatography enantioseparations, J. Chromatogr. A 906 (2001) 253–273.
[13] G. Massolini, E. Calleri, A. Lavecchia, F. Loiodice, D. Lubda, C. Temporini, G. Fracchiolla, P. Tortorella, E. Novellino, G. Caccialanza, Enantioselective hydrolysis of some 2-aryloxyalkanoic acid methyl esters and isosteric analogues using a penicillin G acylase-based HPLC monolithic silica column, Anal. Chem. 75 (2003) 535–542.

[14] E. Calleri, G. Massolini, D. Lubda, C. Temporini, F. Loiodice, G. Caccialanza, Evaluation of a monolithic epoxy silica support for penicillin G acylase immobilization, J. Chromatogr. A. 1031 (2004) 93–100.
[15] E. Calleri, C. Temporini, G. Massolini, G. Caccialanza, Penicillin G acylase-based stationary phases: analytical applications, J. Pharm. Biomed. Anal. 35 (2004) 243–258.
[16] M. Arroyo, I. de la Mata, C. Acebal, M.P. Castillón, Biotechnological applications of penicillin acylases: state-of-the-art, Appl. Microbiol. Biotechnol. 60 (2003) 507–514.
[17] G. Massolini, E. Calleri, E. De Lorenzi, M. Pregnolato, M. Terreni, G. Felix, C. Gandini, Immobilized penicillin G acylase as reactor and chiral selector in liquid chromatography, J. Chromatogr. A 921 (2001) 147–160.
[18] E. Calleri, G. Massolini, F. Loiodice, G. Fracchiolla, C. Temporini, G. Félix, P. Tortorella, G. Caccialanza, Evaluation of a penicillin G acylase-based chiral stationary phase towards a series of 2-aryloxyalkanoic acids, isosteric analogs and 2-arylpropionic acids, J. Chromatogr. A 958 (2002) 131–140.
[19] K. Liu, L. Xu, J.P. Berger, K.L. MacNaul, G. Zhou, T.W. Doebber, M.J. Forrest, D.E. Moller, A.B. Jones, Discovery of a novel series of peroxisome proliferator-activated receptor alpha/gamma dual agonists for the treatment of type 2 diabetes and dyslipidemia, J. Med. Chem. 48 (2005) 2262–2265.
[20] A. Pinelli, G. Godio, A. Laghezza, N. Mitro, G. Fracchiolla, V. Tortorella, A. Lavecchia, E. Novellino, J.C. Fruchart, B. Staels, M. Crestani, F. Loiodice, Synthesis, biological evaluation, and molecular modeling investigation of new chiral fibrates with PPARalpha and PPARgamma agonist activity, J. Med. Chem. 48 (2005) 5509–5519.
[21] M.P. Grella, R. Danso-Danquah, M.K. Safo, G.S. Joshi, J. Kister, M. Marden, S.J. Hoffman, D.J. Abraham, Synthesis and structure–activity relationships of chiral allosteric modifiers of hemoglobin, J. Med. Chem. 4 (2000) 4726–4737.
[22] G. Bettoni, F. Loiodice, V. Tortorella, D. Conte-Camerino, M. Mambrini, E. Ferrannini, S.H. Bryant, Stereospecificity of the chloride ion channel: the action of chiral clofibric acid analogs, J. Med. Chem. 30 (1987) 1267–1270.
[23] A. Liantonio, A. De Luca, S. Pierno, M.P. Didonna, F. Loiodice, G. Fracchiolla, P. Tortorella, A. Laghezza, E. Bonerba, S. Traverso, L. Elia, A. Picollo, M. Pusch, D. Conte-Camerino, Structural requisites of 2-(*p*-chlorophenoxy)propionic acid analogues for activity on native rat skeletal muscle chloride conductance and on heterologously expressed CLC-1, Br. J. Pharmacol. 139 (2003) 1255–1264.
[24] D. Feller, V.S. Kamanna, H.A.I. Newman, K.J. Romstedt, D.T. Witiak, G. Bettoni, S.H. Bryant, D. Conte-Camerino, F. Loiodice, V. Tortorella, Dissociation of hypolipidemic and antiplatelet actions from adverse myotonic effects of clofibric acid related enantiomers, J. Med. Chem. 30 (1987) 1265–1267.
[25] R.D. Larsen, E.G. Corley, P. Davis, P.J. Reider, E.J.J. Grabowski, α-Hydroxy esters as chiral reagents: asymmetric synthesis of 2-arylpropionic acids, J. Am. Chem. Soc. 111 (1989) 7650–7651 (and references therein).
[26] S.H. Done, J.A. Brannigan, P.C. Moody, R.E. Hubbard, Ligand-induced conformational change in penicillin acylase, J. Mol. Biol. 284 (1998) 463–475.
[27] C.E. McVey, M.A. Walsh, G.G. Dodson, K.S. Wilson, J.A. Brannigan, Crystal structures of penicillin acylase enzyme–substrate complexes: structural insights into the catalytic mechanism, J. Mol. Biol. 313 (2001) 139–150.
[28] J.A. Brannigan, G. Dodson, H.J. Duggleby, P.C.E. Moody, J.L. Smith, D.R. Tomchick, A.G. Murzin, A protein catalytic framework with an N-terminal nucleophile is capable of self-activation, Nature 378 (1995) 416–419.
[29] I. Mononen, K.J. Fischer, V. Kaartinen, N.N. Aronson, Aspartylglycosaminuria: protein chemistry and molecular biology of the most common lysosomal storage disorder of glycoprotein degradation, FASEB J. 7 (1993) 1247–1256.
[30] J. Löwe, D. Stock, B. Jap, P. Zwickl, W. Baumeister, R. Huber, Crystal structure of the 20S proteasome from the archaeon T. acidophilum at 3.4 A resolution, Science 268 (1995) 533–539.
[31] J.L. Smith, E.J. Zaluzec, J.P. Wery, L. Niu, R.L. Switzer, H. Zalkin, Y. Satow, Structure of the allosteric regulatory enzyme of purine biosynthesis, Science 264 (1994) 1427–1433.
[32] H.J. Duggleby, S.P. Tolley, C.P. Hill, E.J. Dodson, P.C. Moody, Penicillin acylase has a single-amino-acid catalytic centre, Nature 373 (1995) 264–268.
[33] G. Massolini, G. Fracchiolla, E. Calleri, G. Carbonara, C. Temporini, A. Lavecchia, S. Cosconati, E. Novellino, F. Loiodice, Elucidation of the Enantioselective Recognition Mechanism of a Penicillin G Acylase-Based Chiral Stationary Phase Towards a Series of 2-Aryloxy-2-Arylacetic Acids, Chirality 18 (2006) 633–643.
[34] G.M. Morris, D.S. Goodsell, R.S. Halliday, R. Huey, W.E. Hart, R.K. Belew, A.J. Olson, Docking using a Lamarckian genetic algorithm and an empirical binding free energy function, J. Comp. Chem. 19 (1998) 1639–1662.
[35] D.S. Goodsell, G.M. Morris, A.J. Olson, Automated docking of flexible ligands: applications of AutoDock, J. Mol. Recognit. 9 (1996) 1–5.
[36] J. Marelius, K. Kolmodin, I. Feierberg, J. Åqvist, Q: a molecular dynamics program for free energy calculations and empirical valence bond simulations in biomolecular systems, J. Mol. Graph. 16 (1998) 213–225.
[37] J. Åqvist, C. Medina, J.E. Samuelsson, A new method for predicting binding affinity in computer-aided drug design, Protein Eng. 7 (1994) 385–391.
[38] J. Åqvist, T. Hansson, On the validity of electrostatic linear response in polar solvents, J. Phys. Chem. 100 (1996) 9512–9521.
[39] J. Marelius, T. Hansson, J. Åqvist, Calculation of ligand binding free energies from molecular dynamics simulations, Int. J. Quantum Chem. 69 (1998) 77–88.
[40] F. Osterberg, J. Åqvist, Exploring blocker binding to a homology model of the open hERG K+ channel using docking and molecular dynamics methods, FEBS Lett. 579 (2005) 2939–2944.
[41] J. Hulten, N.M. Bonham, U. Nillroth, T. Hansson, G. Zuccarello, A. Bouzide, J. Åqvist, B. Classon, U.H. Danielson, A. Karlen, I. Kvarnstrom, B. Samuelsson, A. Hallberg, Cyclic HIV-1 protease inhibitors derived from mannitol: synthesis, inhibitory potencies, and computational predictions of binding affinities, J. Med. Chem. 40 (1997) 885–897.
[42] K. Ersmark, M. Nervall, E. Hamelink, L.K. Janka, J.C. Clemente, B.M. Dunn, M.J. Blackman, B. Samuelsson, J. Åqvist, A. Hallberg, Synthesis of malarial plasmepsin inhibitors and prediction of binding modes by molecular dynamics simulations, J. Med. Chem. 48 (2005) 6090–6106.
[43] M. Almlof, J. Åqvist, A.O. Smalas, B.O. Brandsdal, Probing the effect of point mutations at protein–protein interfaces with free energy calculations, Biophys. J. 90 (2006) 433–442.
[44] SYBYL Molecular Modeling System (Version 7.1), TRIPOS Assoc., St. Louis, MO.
[45] J. Head, M.C. Zerner, A Broyden–Fletcher–Goldfarb–Shannon optimization procedure for molecular geometries, Chem. Phys. Lett. 122 (1985) 264–270.
[46] J.G. Vinter, A. Davis, M.R. Saunders, Strategic approaches to drug design. An integrated software framework for molecular modelling, J. Comput. Aided Mol. Des. 1 (1987) 31–51.
[47] J. Gasteiger, M. Marsili, Iterative partial equalization of orbital electronegativity—a rapid access to atomic charges, Tetrahedron 36 (1980) 3219–3228.
[48] F.C. Bernstein, T.F. Koetzle, G.J.B. Williams, E.F.J. Meyer, M.R. Brice, J.R. Rodgers, O. Kennard, T. Shimanouchi, T. Tasumi, The Protein Data Bank: a computer-based archival file for macromolecular structures, J. Mol. Biol. 112 (1977) 535–542.
[49] W.L. DeLano, The PyMOL Molecular Graphics System (2002), http://www.pymol.org.
[50] W.D. Cornell, P. Cieplak, C.I. Bayly, I.R. Gould, K.M. Merz Jr., D.M. Ferguson, D.C. Spellmeyer, T. Fox, J.W. Caldwell, P.A. Kollman, A second generation force field for the simulation of proteins, nucleic acids, and organic molecules, J. Am. Chem. Soc. 117 (1995) 5179–5197.
[51] G. Subramanian, M.G. Paterlini, D.L. Larson, P.S. Portoghese, D.M. Ferguson, Conformational analysis and automated receptor docking of selective arylacetamide-based κ-opioid agonists, J. Med. Chem. 41 (1998) 4777–4789.

[52] A. Jakalian, D.B. Jack, C.I. Bayly, Fast, efficient generation of high-quality atomic charges. AM1-BCC model. II. Parameterization and validation, J. Comput. Chem. 23 (2002) 1241–1623.
[53] W. Wang, W.A. Lim, A. Jakalian, J. Wang, J. Wang, R. Luo, C.I. Bayly, P.A. Kollman, An analysis of the interactions between the Sem-5 SH3 domain and its ligands using molecular dynamics, free energy calculations, and sequence analysis, J. Am. Chem. Soc. 123 (2001) 3986–3994.
[54] W. Jorgensen, J. Chandrasekhar, J.D. Madura, R.W. Impey, M.L. Klein, Comparison of simple potential functions for simulating liquid water, J. Chem. Phys. 79 (1983) 926–935.
[55] T. Hansson, J. Marelius, J. Åqvist, Ligand binding affinity prediction by linear interaction energy methods, J. Comput. Aided Mol. Des. 12 (1998) 27–35.
[56] F.S. Lee, Z.T. Chu, M.B. Bolger, A. Warshel, Calculations of antibody–antigen interactions: microscopic and semi-microscopic evaluation of the free energies of binding of phosphorylcholine analogs to McPC603, Prot. Eng. 5 (1992) 215–228.
[57] G. Götmar, T. Fornstedt, G. Guiochon, Apparent and true enantioselectivity in enantioseparations, Chirality 12 (2000) 558–564.
[58] M. Guncheva, I. Ivanov, B. Galunsky, N. Stambolieva, J. Kaneti, Kinetic studies and molecular modeling attribute a crucial role in the specificity and stereoselectivity of penicillin acylase to the pair ArgA145–ArgB263, Eur. J. Biochem. 271 (2004) 2272–2279.
[59] C.A. Hunter, Arene–arene interactions: electrostatic or charge transfer? Angew. Chem. Int. Ed. Engl. 32 (1993) 1584–1586.
[60] F.J. Cozzi, S. Siegel, Interaction between stacked aryl groups in 1,8-diarylnaphthalenes: dominance of polar/π over charge-transfer effects, Pure Appl. Chem. 67 (1995) 683–689.
[61] S.B. Ferguson, E.M. Sanford, E.M. Seward, F. Diederich, Cyclophane–arene inclusion complexation in protic solvents: solvent effects versus electron donor–acceptor interactions, J. Am. Chem. Soc. 113 (1991) 5410–5419.
[62] S. Raza, L. Fransson, K. Hult, Enantioselectivity in *Candida antarctica* lipase B: a molecular dynamics study, Protein Sci. 10 (2001) 329–338.